J. Am. Soc. Mass Spectrom. (2017) 28:2384–2392
DOI: 10.1007/s13361-017-1747-3

RESEARCH ARTICLE

On the Nature of Mass Spectrometer Analyzer Contamination

Yang Kang, Bradley B. Schneider, Thomas R. Covey

SCIEX, 71 Four Valley Drive, Concord, ON L4K 4V8, Canada

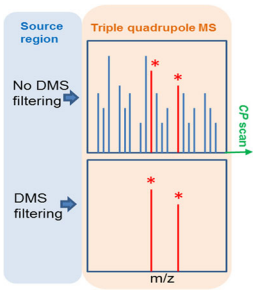

Abstract. Sample throughput in electrospray ionization mass spectrometry (ESI-MS) is limited by the need for frequent ion path cleaning to remove accumulated debris that can lead to charging and general performance degradation. Contamination of ion optics within the vacuum system is particularly problematic as routine cleaning requires additional time for cycling the vacuum pumps. Differential mobility spectrometry (DMS) can select targeted ion species for transmission, thereby reducing the total number of charged particles entering the vacuum system. In this work, we characterize the nature of instrument contamination, describe efforts to improve mass spectrometer robustness by applying DMS prefiltering to reduce contamination of the vacuum ion optics, and demonstrate the capability of DMS to extend the interval between mass spectrometer cleaning. In addition, we introduce a new approach to effectively detect large charged particles formed during the electrospray ionization (ESI) process.

Keywords: DMS prefiltering, Contamination, Clusters, Robustness

Received: 30 March 2017/Revised: 20 June 2017/Accepted: 20 June 2017/Published Online: 21 July 2017

Introduction

Electrospray ionization-mass spectrometry (ESI-MS) is a well-established technique for routine analysis of complex mixtures, widely applied in pharmaceutical and biotech applications [1]. High-throughput analysis of complex samples, however, is challenging due to the existence of complex background matrix [2, 3]. Analytical signals from the background matrix, generally referred to as "chemical noise," can degrade the signal to noise ratio (S/N) and contribute to contamination of the ion optics of a mass spectrometer because of the impaction of charged ions and particles with various lens elements. It is particularly problematic when severe contamination of the vacuum ion optics elements of a mass spectrometer occurs, as routine cleaning requires additional time for cycling the vacuum pumps; this limits the sample throughput and analysis efficiency.

Commonly observed chemical noise in mass spectra is solvent-induced ions produced during ESI processes [3–5], typically at high abundance and primarily having a mass to charge ratio (m/z) less than 300 [5]. When the ion of interest has a similar m/z to the interference ions, a reduction in S/N and quantitation accuracy can occur [6], with the increased complexity complicating spectral interpretation. In addition to low-mass solvent-derived ions, "soft" ionization approaches such as ESI may generate large ion cluster complexes [7, 8], such as oligosaccharide aggregation [9], peptide aggregation, and protein complexes interacting with a variety of molecules [10, 11]. Ions of interest may be encapsulated within large heterogeneous clusters. These complex and unresolved mixtures can have m/z exceeding the mass range of a typical triple quadrupole instrument, and therefore they are difficult to detect using current commercially available MS techniques. However, larger clusters can contribute to chemical noise, particularly when analyzing high-concentration solutions [12] or incorporating liquid chromatography (LC) [13]. Furthermore, these large clusters may have multiple charges, and penetrate into downstream ion optics as far as the detector, leading to charging and contamination. Overall, both low-mass and high-mass solvent- or matrix-induced materials are contributors to vacuum contamination, leading to charging and general performance degradation.

Accordingly, robust and practical methods and systems that enable the analysis of increasingly complex samples, with reduction or elimination of contamination caused by unwanted materials, are in high demand. This has driven the development of post-ESI separation techniques to prevent both neutrals and charged ions or particles from entering the MS vacuum system. For example, the bulk of solvent or large droplets from an ESI plume can be directed into the exhaust when positioning the ionization sprayer in off-axis [13] or orthogonal orientation

Correspondence to: Yang Kang; *e-mail:* yang.kang@sciex.com

[14] from the vacuum inlet. Neutrals and clusters can be effectively reduced by facilitating declustering and desolvation processes, with application of counter-current inert drying gas (curtain gas [13]), auxiliary heated drying gas, or placing heated elements between the ion source and vacuum inlet such as a heated metal capillary [15]. Large particles or solvent clusters can also be removed from the gas beam by a skimmer cone [16] or a laminar flow chamber acting as a particle discriminator [17, 18]. In addition to developments in the atmospheric pressure region, modifications to the ion optics in the vacuum region have also been developed to prevent neutrals and large clusters from entering the next stage of the mass spectrometer to reduce mass analyzer contamination. Examples include shifting the entrance ion optics off axis [19, 20] from the sampling aperture, using a curved quadrupole ion guide [21, 22], and heating the first entrance electrode [23]. All of these methods focus on elimination of neutrals and heavy droplets or clusters.

Alternatively, ion mobility-based techniques [5, 24] such as differential mobility-based ion selection can be used to eliminate unwanted charged debris prior to the vacuum inlet. Unlike conventional ion mobility spectrometers that use drift time to distinguish ions under a low electric field [25], differential mobility spectrometry takes advantage of the field dependence of ion mobility; strong electric fields are used to select targeted species prior to the mass spectrometer inlet. A standard design currently available in commercial devices uses two parallel plate electrodes interfaced to a mass spectrometer inlet [26]. The unique separation in DMS is dependent on various ion characteristics, including mass, charge, size, conformation, ion–molecule interaction, or other ion properties such as molecular polarizability, making it possible to distinguish target species from different kinds of background chemical noise. When compared with the use of MS alone, DMS prefiltering has demonstrated significantly decreased chemical noise, leading to improved S/N and enhanced quantitative accuracy [27]. Some examples include detection of small molecule metabolites with high chemical interference [6] and analysis of steroids with poor ionization efficiency [28, 29].

The theory and operational principles of DMS have been described in detail elsewhere [26, 30, 31]. In general, ions are separated based on their mobility difference between high and low electric fields by the application of a periodic asymmetric separation field. Differences in mobility over each period of the waveform cause ions to be displaced towards the electrodes. The ion trajectory can be counterbalanced with a weak DC compensation voltage (*CoV*). When the *CoV* is set to the appropriate value to counteract the unique differential mobility of a particular ion, a continuous ion beam passes to the mass spectrometer for that species. This mode of operation is typical for the analysis of targeted chemical species with known *CoV*. Alternatively, the *CoV* can be ramped to sequentially pass ions that have a broad range of *CoV* values. This mode of operation is typically used for the analysis of unknown chemical species.

In this study, we characterize the nature of mass spectrometer contamination by comparing the extent of instrument contamination (signal loss and visible debris deposits) for highly accelerated robustness tests conducted under standard instrument conditions and while using a DMS to extract charged species prior to the inlet orifice. When comparing the results, it is possible to determine the relative contributions of neutrals versus charged species for instrument contamination. Additionally, we describe a new acquisition approach to detect the presence of ions or charged particles with *m/z* greater than the mass range of a typical triple quadrupole instrument, hereafter referred to as "charged particle" (*CP*) scan. The mobility behavior of large *m/z* species, formed from various matrices, is studied, and it is shown that a DMS device can effectively remove these large charged ions or particles prior to the mass spectrometer inlet. This approach may be particularly advantageous for peptide analysis, as DMS devices can selectively remove both singly charged low *m/z* ion current and high *m/z* species. It is shown that DMS prefiltering can reduce the contamination of vacuum ion optics, enhancing mass spectrometer robustness.

Experimental

Experiments were conducted using a hybrid triple quadrupole (QqQ)/linear ion trap mass spectrometer (QTRAP® 6500; SCIEX, Concord, ON, Canada) outfitted with a standard DMS system (SelexION® Technology; SCIEX). Ions were generated with a standard Turbo V™ ion source. The standard DMS electrodes were mounted within the curtain chamber of the instrument and sealed to the vacuum inlet orifice [7, 26, 31]. Nitrogen was used as the transport gas flowing through the cell at approximately 4 L/min, drawn from the curtain chamber by the vacuum drag through the inlet orifice (~0.72 mm). The DMS heat exchanger temperature was set to 150 °C unless otherwise specified. Ionograms were collected by ramping the *CoV* at a fixed separation voltage (*SV*) applied between the DMS electrodes. Data were acquired using Analyst® software (SCIEX). For *CP* scan experiments, the system was modified to permit the first mass analyzing quadrupole (Q1) to operate in rf-only mode with a low mass cut-off of approximately 1550 Da.

For experiments with bovine serum albumin (BSA) digest, a total of 56 multiply charged peptides (*m/z* range from 330 to 840) were analyzed in multiple reaction monitoring (MRM) mode while scanning the DMS compensation voltage. The dwell time was 50 ms for each transition. For each peptide ion, the highest-intensity fragment ion with *m/z* greater than the corresponding parent ion was selected with optimized collision energy (CE). Ionograms of these peptides were generated by ramping *CoV* values in steps of 0.2 V over a range of −10 V to 45 V at a fixed *SV* of 4250 $V_{p\text{-}p}$ (~148 Td). In addition, ionograms of 18 singly charged ions generated from the same BSA sample were collected as well. These ions had high abundance and a wide *m/z* range from 250 to 930. The BSA digest was infused at a flow rate of 10 μL/min.

Highly Accelerated Robustness Testing

Test 1: Concentrated olive oil solution comprising ~3 mM lipids was infused at a flow rate of 10 μL/min continuously with the curtain gas set to 20 psi for 120 h, with and without DMS installed. When the DMS was installed, the experiments were conducted with the *SV* set to 3500 V (~122 Td) and the *CoV* set to 100 V to filter out all charged species.

Test 2: Concentrated Hank's buffer solution was infused at a flow rate of 100 μL/min for 24 h, using a 100 mL syringe (Gastight 1000; Hamilton Company, Reno, NV, USA) and a syringe pump (Harvard Apparatus, Holliston, MA, USA). When the DMS was installed, the experiments were conducted with the *SV* and *CoV* set for multiply charged peptide analysis (*SV* = 4000 V, ~139 Td, and *CoV* = 25 V).

Test 3: Concentrated human plasma solution was infused at a flow rate of 1 μL/min continuously for 4 days using a NanoSpray® III source (SCIEX). The nanoflow sprayer had a 20 μm i.d., pulled to 10 μm at the tip (part number FS360-20-10-N-20-C12; New Objectives, Woburn, MA, USA). When the DMS was installed, the experiments were conducted with the *SV* and *CoV* set to 3500 V and 20 V, respectively.

The performance of the system was monitored by periodically measuring the MRM signal of reserpine ions (*m/z* 609.3) from a 10 pg/μL reserpine solution. Various ion optics elements were examined for the presence of visible debris, and photographed after each contamination experiment.

Chemicals and Reagents

The solutions used for *CP* scans were prepared with reserpine diluted in three solvent matrices; 100 pg/μL in a solvent mixture containing ethanol, methanol, water, isopropanol, and formic acid with volume ratio of 22:51:33:1:0.1, 100 pg/μL in acetonitrile precipitated (crashed) horse plasma, and 10 ng/μL in Hank's buffer. Concentrated lipid solutions were made from a sample of extra virgin olive oil diluted by 1000× in solvent comprising 1:1 methanol:methylene chloride with 5 mM ammonium acetate. Hank's buffer solution was prepared using the manufacturer's specified procedure without further dilution. Human plasma (BioreclamationIVT, Westbury, NY, USA) was acetonitrile-precipitated without further dilution. BSA protein was trypsin-digested following a standard procedure [32], to produce stock solutions containing 30 pmol/μL of digested BSA, which were then frozen at −20 °C in aliquots. Prior to analysis, each BSA stock solution was diluted to 100 fmol/μL in solvent comprising 50/50 water/methanol (v/v) with 0.1% formic acid.

Reserpine, BSA, horse plasma, Hank's buffer, and formic acid were purchased from Sigma-Aldrich Co. (St. Louis, MO, USA). Methanol, acetonitrile, and isopropanol were purchased from Caledon Laboratories Ltd. (Georgetown, ON, Canada). Ethanol was purchased from Avantor Performance Materials, Inc. (Center Valley, PA, USA).

Results and Discussion

The mass spectrometer used for these studies had the general interface configuration shown in Figure 1, and ions were generated by ESI using an orthogonal sprayer configuration. Ions and charged droplets were exposed to a counter-current "curtain gas" [13] as they passed through a curtain plate prior to the inlet orifice. The first vacuum stage was pumped to approximately 2 Torr and contained a rf-only quadrupole to focus ions through a lens (labeled IQ0) prior to the second differentially pumped vacuum stage. The second vacuum stage included an additional rf-only quadrupole to focus ions through the IQ1 lens prior to the mass analyzer region. Optionally, a DMS cell could be mounted in the region between the curtain plate and orifice plate to provide filtering of charged species prior to the inlet orifice. When running highly complex samples, contamination has been observed on all of the lenses preceding the mass analyzer. A series of experiments were conducted to characterize the nature of mass spectrometer contamination. Concentrated lipid solutions were sprayed for 120 h with no DMS installed, as described in more detail under the preceding section with regard to *highly accelerated robustness Test 1*. Table 1 shows the measured ion current (RSD of ~2%) initially and after 120 h of infusion of the lipid solution. The signal for a reserpine standard decreased by a factor of 2 when no DMS was present on the system, and the reason for this decrease is evident in the three pictures at the top of Figure 1. A substantial portion of debris accumulated on a number of the lenses, including the curtain plate, IQ0, and IQ1. After cleaning the lens elements of this system one at a time, it was apparent that the greatest contributors to signal loss were debris accumulated on the inlet orifice and the IQ1 lens.

The electrospray process generates ions as well as highly charged droplets. The desolvation process may also release solvent clusters. The orthogonal spray geometry and curtain gas flow help to minimize the penetration of neutral species into the vacuum system; however, the presence of neutrals cannot be ruled out entirely. Therefore, to help characterize the nature of contaminating materials present on ion path elements, the highly accelerated contamination test was repeated with a DMS installed. For these experiments, the DMS was operated with an uncharacteristically high *CoV* to substantially block all of the ion current prior to the inlet orifice (*SV* = 3500 V and *CoV* = 100 V). While this mode of operation is completely impractical since ion analysis is not possible, it provides a means to differentiate between contamination resulting from charged species and neutrals. When the DMS was enabled, the ion current measured in a Q1 scan dropped from 3.09×10^9 cps to 513 cps, demonstrating almost complete elimination of any charged species within the ion path. Under these conditions, there was no change in the measured intensity

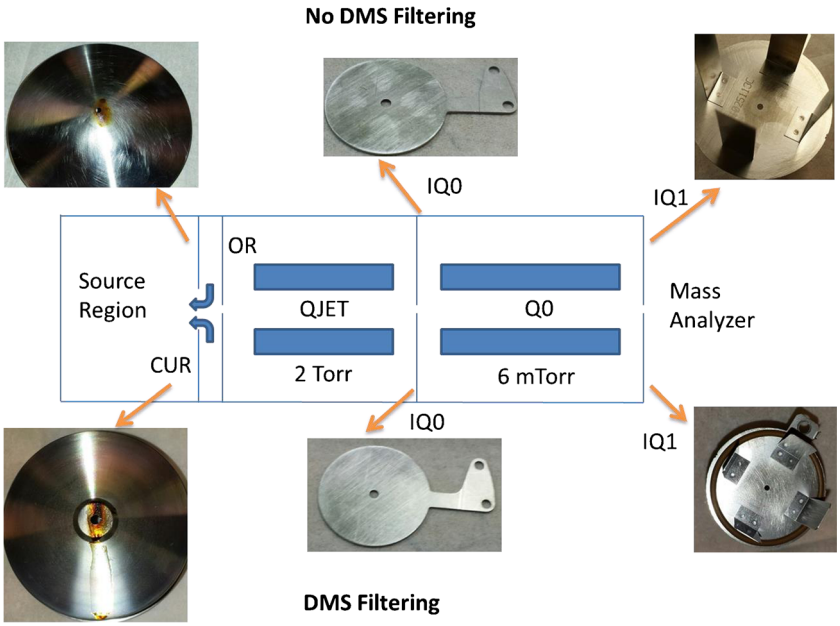

Figure 1. Schematic of the mass spectrometer system used for these studies. Ions were generated by electrospray ionization in a source region. They passed through a counter-current flow of nitrogen directed by a curtain plate (CUR) prior to entering the mass spectrometer inlet orifice (OR). The system was differentially pumped, and a quadrupole ion guide was installed in the first vacuum stage (QJET). The ions passed through an aperture (IQ0) prior to the second differentially pumped vacuum stage. The second vacuum stage included an additional quadrupole ion guide (Q0), and an additional aperture (IQ1) was located prior to the first quadrupole mass analyzer. The digital photographs across the top of Figure 1 show three of the ion path elements (CUR, IQ0, and IQ1) after a highly accelerated robustness test that involved infusion of concentrated lipid solution for 120 h. The digital photographs across the bottom of Figure 1 show the same ion path elements after the same highly accelerated robustness test conducted with a DMS installed between the curtain plate and orifice

for reserpine ions from the start of the experiment to the end of the 120 h interval (Table 1). The digital photographs in the bottom of Figure 1 show the same ion path elements as discussed previously; a visual comparison of the pictures on the top and bottom of Figure 1 shows that charged species are the principal contributors to instrument contamination. The curtain plate is located prior to the DMS, so it is exposed to a similar quantity of charged debris regardless of whether or not the DMS is enabled. Therefore, as expected, a large quantity of debris was present on the surface of the curtain plate for both experiments. However, the ion path lens elements, IQ0 and IQ1, showed no visible debris deposits at all after 120 h when the DMS filtered all charged species prior to the inlet orifice. Given that the DMS cannot filter neutrals, these data provide powerful evidence that the material that contributes to mass spectrometer ion path contamination and, hence, signal degradation is charged species from the ion source region.

The nature of contaminating material can be further confirmed by filtering charged species in other regions of the mass spectrometer. The simplest way to control the ion current is to use the ESI potential. Highly accelerated contamination tests were conducted by continuously infusing concentrated Hank's buffer solution at a flow rate of 100 µL/min for 24 h as described previously under *highly accelerated robustness Test 2*. This sample contains an excessive amount of salt, and tends to plug apertures when sprayed without dilution. For these experiments, the DMS was removed from the instrument. Initially the Hank's buffer sample was sprayed under typical conditions (ion spray voltage applied), with a higher curtain gas flow (9.5 L/min) and with the source heaters set to 500 °C to assist desolvation. As shown in Figure 2a, orifice blockage was observed in 14 h, despite operating with a relatively high curtain gas setting. Charged species penetrated through the counter-current gas flow and near complete blockage of the orifice limited the gas flow into the vacuum system, resulting in system shutdown attributable to a low base pressure error. Visible contamination was also present on downstream lens elements. The curtain plate, orifice, and vacuum lens elements had to be cleaned to restore system performance. The Hank's buffer experiment was repeated with the ion spray voltage turned off to eliminate electrospray charging of the sample liquid; neutrals were the predominant species generated under these conditions. Although it is possible that some statistical charging may still be expected, the very low efficiency of this process essentially eliminated all signal in the mass spectrometer. With the ion spray voltage turned off, a large amount of

Table 1. Reserpine Count Rates for 120 h Lipid Infusion Experiments

	No DMS	DMS blocking charged species
Initial baseline (cps)	3.8×10^5	4.2×10^5
Final baseline (cps)	1.8×10^5	4.2×10^5
Signal decrease	2.1X	0X

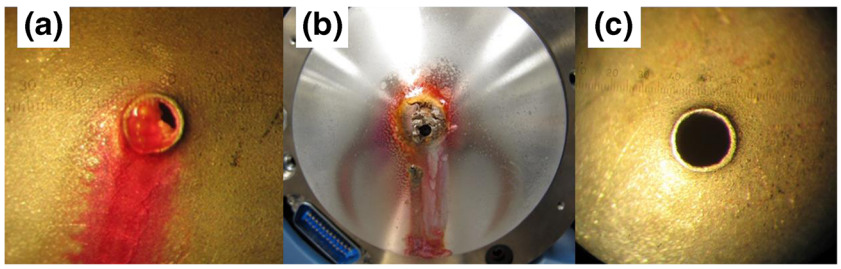

Figure 2. Digital photographs of ion path elements after continuous infusion of Hank's buffer for 24 hours. (**a**) Inlet orifice after experiments with the ion spray voltage on, (**b**) curtain plate after experiments with the ion spray voltage off, and (**c**) inlet orifice after experiments with the ion spray voltage off

debris was present on the curtain plate (Figure 2b), and this was similar to what was observed for the previous experiment where the ion spray voltage was on. This is not surprising, given that the nebulizer gas flow is the key determinant for spray plume shape. With the ion spray voltage turned off, the curtain gas flow effectively blocked neutral species from entering the curtain plate aperture, and this ensured that the orifice (and all downstream lens elements) did not become visibly contaminated. A comparison of the digital photographs of the orifice shows a striking reduction in visible contamination for the experiment where the ion spray potential was turned off (Figure 2c). These results clearly support the premises that neutral species are effectively blocked by a curtain gas configuration and charged species from the source region are predominantly responsible for ion path contamination.

Charged contamination in mass spectrometry is inevitable when using nonspecific ionization processes such as ESI, MALDI, or APCI. For targeted quantitation approaches, any signal visible in the spectra other than the compound of interest can be considered to be charged contamination. This includes the typical high intensity, low *m/z* peaks generated by ESI, as well as other contaminants from the environment such as phthalates and silicones, and peaks from species present in the solvent matrix [3]. For instance, the signal for the ion of interest was typically in a range of 10^3 to 10^7 cps, while the total ion current could be on the order of 10^{10} cps. In such cases, the target sample comprises only a small portion of the total ion current. Sources of low *m/z* contamination are well known and frequently described in the literature [3–5]; however, they are not the only contributors to contamination. Ion path contamination may also occur because of large charged species, which may comprise highly charged droplets or clusters. These species are not typically considered because they may have *m/z* values greater than the mass range of typical triple quadrupole instruments, rendering them effectively invisible to quadrupole systems that operate with typical scan modes.

A custom triple quadrupole scan was used to look for the presence of large charged species from a reserpine sample which was prepared in a solvent mixture as described in "-*Chemicals and Reagents*" section. The first mass analyzing quadrupole of the system was operated in rf-only mode, and the low mass cut-off was set to approximately 1550 Da. Under these conditions, only ions and charged species with *m/z* greater than 1550 passed through Q1 and were transmitted to the collision cell (q2). When the collision energy (CE) for the collision cell was low (5 eV), a scan of Q3 shows the presence of no low *m/z* ion current, and minimal chemical noise in the higher *m/z* range of 1550–2000, as shown in Figure 3a. The presence of large charged species can be demonstrated by increasing the CE to induce fragmentation, while scanning Q3. When the collision energy was increased to 50 eV, larger *m/z* species could be fragmented to liberate reserpine ions as shown in Figure 3b. In this case, a strong signal was observed for reserpine ions liberated from larger charged particles. The presence of reserpine ions demonstrates that though Q1 was set to filter reserpine precursor ions and other ions having *m/z* less than about 1550, a substantial amount ($>1.5\times10^5$ cps) of reserpine ions were liberated from larger charged droplets or clusters. From comparisons of reserpine intensity measured using *CP* scans and normal triple quadrupole scans, we estimate that the fraction of reserpine ions trapped in larger clusters may be as high as 4%. Species with $m/z > 2000$ cannot be detected using a standard quadrupole acquisition approach; thus, they are likely to be ignored or underestimated. However, our *CP* scan results demonstrate that these high-mass charged materials formed during ESI enter the vacuum chamber with a non-negligible quantity. The presence of such massive charged residues may not only degrade the S/N by generating unwanted, unexpected, or interfering product ions, but also generate high ion current to contaminate critical components of the mass spectrometer ion path.

To investigate the capability of DMS prefiltering to remove large charged materials, it is important to determine the mobility behavior of the high *m/z* species generated from different matrices in ESI. Three matrices selected in this work were a solvent mixture with compositions described in "*Chemicals and Reagents*" section, crashed horse plasma, which contains large quantities of organic materials, and Hank's buffer, which is a salt-enriched sugar mixture that contains substantial quantities of inorganic materials. Reserpine standards were spiked into these three matrices, and the intensity of large charged materials was determined by the signal of reserpine ions in Q3 after *CP* scan fragmentation. The optimal collision energy to liberate reserpine ions differed with solvent composition, with 50, 45, and 90 eV required for water/organic mix, Hank's buffer, and crashed plasma,

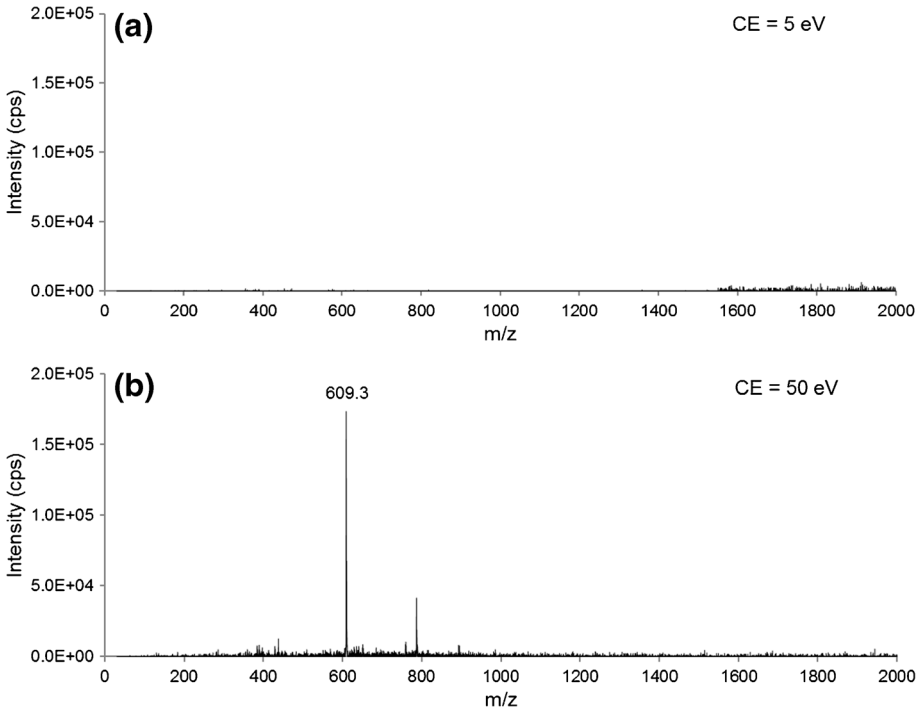

Figure 3. Product ion scans of a sample containing 100 pg/μL of reserpine (*m/z* 609.3), with Q1 filtering out ions having *m/z* less than ~1550 Da, and with the collision energy (CE) in q2 set to (**a**) 5 eV and (**b**) 50 eV

respectively. Figure 4 shows the optimal *CoV* values for the dominant mobility peaks of large charged species from different matrices with increasing separation voltage from 0 to 4250 V. In general, all charged particles, regardless of solvent composition, exhibited Type C behavior (*CoV* increases with increasing separation field), and no peaks were observed in the negative *CoV* region. As expected, charged particles generated from different matrices did not exhibit identical differential mobility. The spread in *CoV* values was approximately 5 V for charged particles generated from different solvents (*SV* = 4250 V).

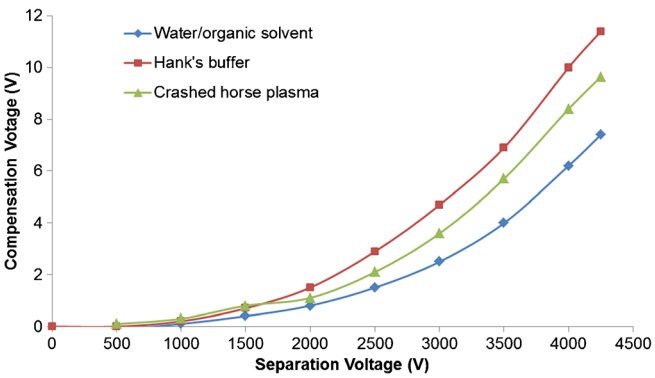

Figure 4. Comparison of *CoV* dependence on separation voltage for large charged species generated from three reserpine-containing solutions, with blue, red, and green traces corresponding to reserpine in the solvent mixture, reserpine in Hank's buffer, and reserpine in crashed horse plasma, respectively

The optimized *CoV* range to transmit large charged materials through the DMS cell overlaps with the range where smaller, singly charged ions would transmit. This can be visualized in the plot of Figure 5, where ionogram peaks for singly, doubly, triply, and quadruply charged ions are displayed. These data were acquired from a sample of BSA digest with the separation voltage set to 4250 V. The bulk of singly charged ions from this sample had optimal *CoV* values ranging from about 5 to 12 V. Conversely, multiply charged peptide ions transmitted with substantially higher *CoV* values (15 to 35 V). Most of the doubly charged peptide ions transmitted with optimum *CoV* values ranging from 16 to 22 V, whereas peptide ions with three charges or more transmitted in a higher *CoV* region, ranging from 18 to 33 V. The tendency for DMS or FAIMS devices to transmit multiply charged ions with higher *CoV* values than singly charged ions has been noted previously [33]. The optimal *CoV* range for large charged species is most consistent with the values used to transmit singly charged ions, and these data suggest that DMS filtering would be able to resolve peptide peaks from both singly charged chemical noise and large charged particles. The flexibility to operate DMS at a fixed *CoV* or stepping the *CoV* across a range enables both quantitative and qualitative peptide analysis while filtering low-mass singly charged ions and high-mass charged droplets or clusters.

Examples of Improved Robustness with DMS Filtering

The Hank's buffer infusion experiment described previously with regard to Figure 2 was repeated with the DMS installed

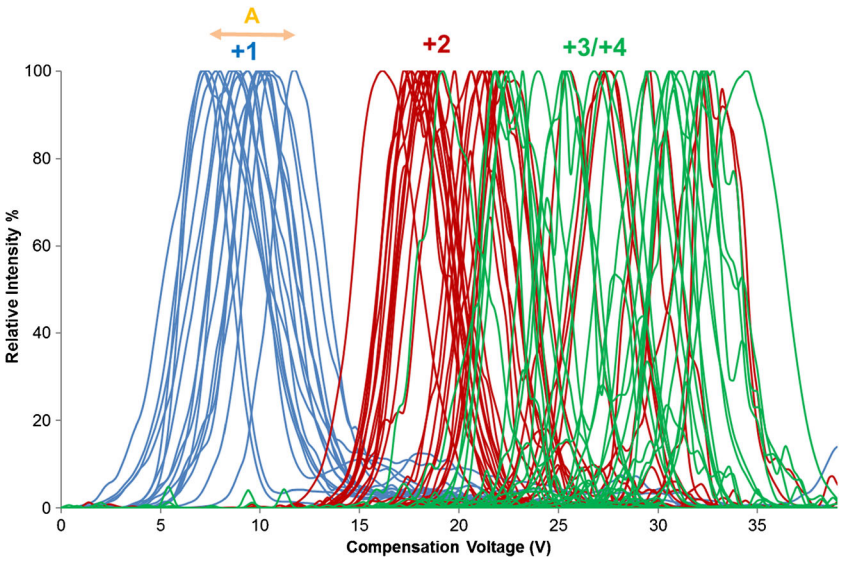

Figure 5. Ionograms of multiply charged peptides (+2 in red, +3/+4 in green), and singly charged ions (blue) from a sample of BSA digest, with *SV* = 4250 V. Singly charged species and large charged materials (region labeled A) transmitted with optimal *CoV* values less than 15 V, whereas multiply charged peptide species typically optimized with *CoV* values greater than 15 V

and set to transmit peptides with predominantly 3+ and 4+ charge states (*CoV* = 25 V and *SV* = 4000 V) to determine the extent of robustness improvement that might be possible for peptide analysis. Based upon the data presented in Figure 5, this mode of operation was expected to completely eliminate singly charged species as well as large charged particles. The DMS protected the downstream orifice, significantly improving instrument robustness, as the orifice was free of visible contamination after 24 h of contamination testing (Figure 6a). In this case, DMS filtering of singly charged species and large charged particles provided similar protection of the inlet orifice and vacuum system as was achieved by turning off the ion spray voltage (Figure 2c). The bulk of debris was deposited onto the DMS electrodes as shown in Figure 6b, eliminating propagation of this material to the downstream lens elements. The materials accumulated on the DMS plates resulted in a sensitivity decrease by ~1.6×, with no substantial effects on the DMS ionogram peak shapes and widths. System performance was fully recovered by cleaning the DMS electrodes and curtain plate only, while the orifice and other downstream lens elements in the vacuum region were not significantly affected. These results suggest that DMS devices can protect the vacuum system of a mass spectrometer when operating with complex samples.

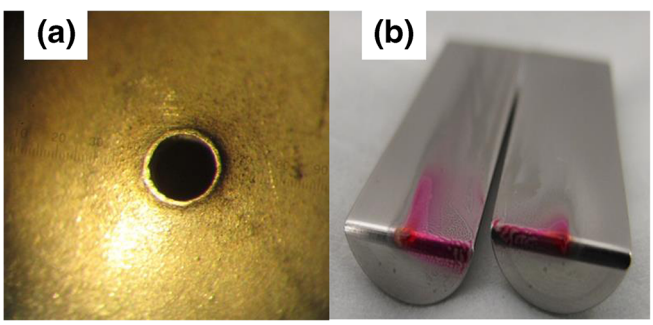

Figure 6. Digital photograph of (**a**) the inlet orifice, and (**b**) the DMS electrodes, after 24 h of infusion of Hank's buffer with a DMS filtering singly charged species and large charged materials from the solution

The general applicability of DMS filtering for contamination reduction was further verified using a crashed plasma matrix and nanoflow interface [17, 32]. Nanoflow ESI interfaces are generally designed to consume the entire electrospray plume, and therefore can represent a worst-case-scenario for instrument contamination. A concentrated crashed human plasma sample was infused continuously at a flow rate representing the upper range of the nanoflow regime (1 μL/min) for 4 days, with and without DMS protection, as described under *highly accelerated robustness Test 3*. Signal degradation was tracked by periodic infusion of a sample of reserpine. In the absence of DMS protection, the reserpine signal was initially 1.0×10^6 cps for reserpine daughter ions, and a signal degradation of 7.7× was observed after 4 days of continuous nanoflow infusion of crashed plasma. The reason for the decay is apparent when looking at the digital photographs in Figures 7a–d, which show the mass spectrometer inlet, QJET, IQ0 lens, and IQ1 lens, respectively. A substantial amount of debris was sampled into the mass spectrometer leaving visible deposits from the inlet to the mass analyzer. Table 2 shows the restoration of signal intensity for reserpine ions achieved by cleaning the ion path one element at a time. Cleaning of the atmospheric pressure components, including the curtain plate, heated inlet, and orifice restored a factor of 2 for reserpine ion intensity; however, the signal was still down by 3.8×. Full recovery of the signal to the initial level required cleaning all of the vacuum lens elements up to the mass analyzer.

The nanoflow infusion experiments were repeated with a DMS installed instead of the standard heated inlet, and the *CoV*

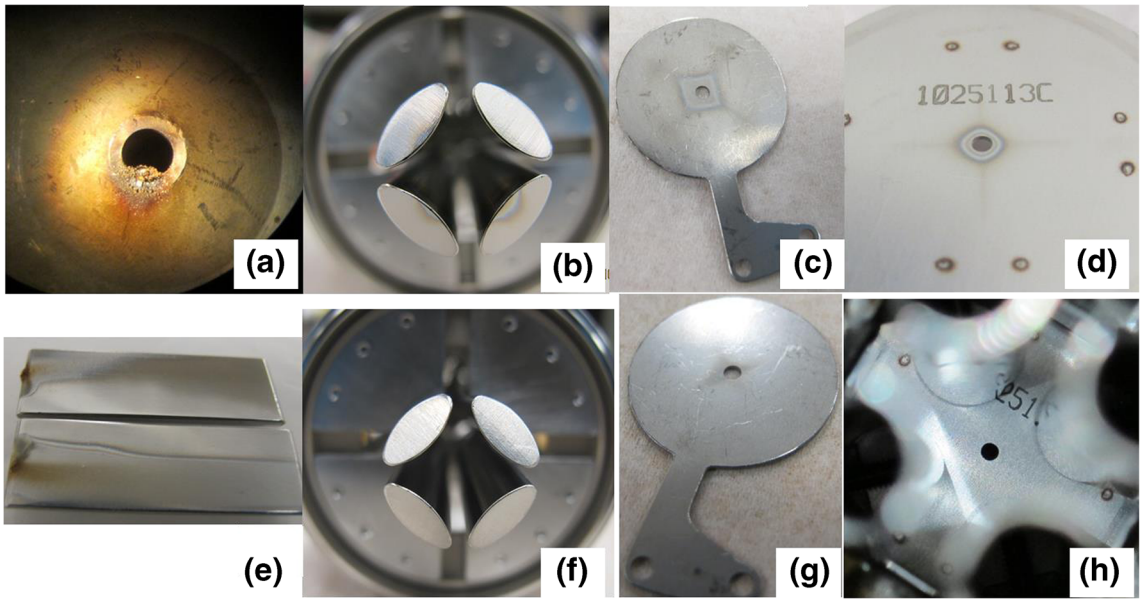

Figure 7. Digital photographs of ion path components after running nanoflow experiments for 4 days with crashed plasma samples with a standard nanoflow interface (**a**)–(**d**) and a DMS interface to electrically protect the vacuum optics (**e**)–(**h**); (**a**) heated inlet, (**b**) entrance of the QJET, (**c**) IQ0 lens, (**d**) IQ1 lens, (**e**) DMS electrodes, (**f**) entrance of the QJET, (**g**) IQ0 lens, and (**h**) IQ1 lens

was set to 20 V (*SV* = 3500 V) to transmit multiply charged peptides while eliminating singly charged chemical background and large charged species. The initial signal for reserpine ions was slightly lower than the standard configuration (4.1×10^5 cps) as expected from previous work [31]. As described in Table 2, much less signal degradation (1.6×) was observed for reserpine ions when the crashed plasma was prefiltered by the DMS device prior to the vacuum system. More importantly, the entire original signal could be restored simply by cleaning the curtain plate and DMS electrodes. None of the lens elements after the DMS had to be cleaned to achieve complete signal restoration. Figures 7e–h show digital photographs of the DMS electrodes, QJET, IQ0, and IQ1 lenses, respectively. The DMS electrodes acted as sacrificial lenses, preventing the bulk of debris from penetrating into the vacuum system of the mass spectrometer. The total accumulation of material on the vacuum lens elements was substantially less when the DMS was in place, and these visual and experimental results confirm the value of DMS prefiltering to reduce system contamination from charged products of atmospheric pressure ionization.

Conclusion

Charged materials from the electrospray process provide the most significant contribution to mass spectrometer ion optics contamination. The unconventional *CP* scan approach described in this paper provides a different view of ESI processes by revealing populations of massive charged ions or particles that would normally not be detected with conventional mass spectrometry approaches. The mobility behavior of large clusters differed with composition of the electrospray solvent; however, much like singly charged noise, large charged species generally transmitted over a characteristic region of *CoV* space that was significantly different than multiply charged peptides. Therefore, DMS shows great potential to be an effective prefilter for peptide analysis. High-mass charged particles and

Table 2. Instrument Signal Recovery for a Reserpine Standard After 4 days of Crashed Plasma Infusion

	Cleaning of ion optics elements				
No DMS	Curtain plate	Aperture on heater plate	Orifice	Vacuum optics	Intensity (cps) of reserpine ion
Initial baseline 1.0×10^6	X	X	X	X	1.3×10^5
	✓	X	X	X	1.3×10^5
	✓	✓	X	X	2.2×10^5
	✓	✓	✓	X	2.6×10^5
	✓	✓	✓	✓	1.0×10^6
DMS with *SV* on	Curtain plate	DMS electrodes	Orifice	Vacuum optics	
Initial baseline 4.1×10^5	X	X	X	X	2.6×10^5
	✓	X	X	X	2.7×10^5
	✓	✓	X	X	4.1×10^5
	✓	✓	✓	X	4.1×10^5
	✓	✓	✓	✓	4.1×10^5

other unwanted singly charged ions could be filtered out with little interference to peptide transmission, providing a cleaner background and improving S/N to enhance the quality and quantitative accuracy of peptide analysis. DMS prefiltering can prevent unwanted charged materials from entering the vacuum system of a mass spectrometer, improving the robustness by reducing the need for cleaning of the ion path elements. Charged particles are deflected to noncritical surfaces located in the atmospheric region of the instrument, where they can be easily accessed and cleaned. Although the signal loss in DMS is generally small, future efforts will be focused on improving transmission to eliminate losses.

Acknowledgements

The authors appreciate the help of Deolinda Fernandes for the preparation of the samples.

References

1. Geoghegan, K.F., Kelly, M.A.: Biochemical applications of mass spectrometry in pharmaceutical drug discovery. Mass Spectrom. Rev. **24**, 347–366 (2005)
2. Domon, B., Aebersold, R.: Mass spectrometry and protein analysis. Science **312**, 212–217 (2006)
3. Keller, B.O., Sui, J., Young, A.B., Whittal, R.M.: Interferences and contaminants encountered in modern mass spectrometry. Anal. Chim. Acta **627**, 71–81 (2008)
4. Handy, R., Barnett, D.A., Purves, R.W., Horlick, G., Guevremont, R.: Determination of nanomolar levels of perchlorate in water by ESI-FAIMS-MS. J. Anal. At. Spectrom. **15**, 907–911 (2000)
5. Menlyadiev, M.R., Tadjimukhamedov, F., Tarassov, A., Wollnik, H., Eiceman, G.A.: Low-mobility-pass filter between atmospheric pressure chemical ionization and electrospray ionization sources and a single quadrupole mass spectrometer: computational models and measurements. Rapid Commun. Mass Spectrom. **28**, 135–142 (2014)
6. Jasak, J., Blanc, Y.L., Speer, K., Billian, P., Schoening, R.M.: Analysis of triazole-based metabolites in plant materials using differential mobility spectrometry to improve LC/MS/MS selectivity. J. AOAC Int. **95**, 1768–1776 (2012)
7. Schneider, B.B., Covey, T.R., Coy, S.L., Krylov, E.V., Nazarov, E.G.: Control of chemical effects in the separation process of a differential mobility mass spectrometer system. Eur. J. Mass Spectrom. **16**, 57–71 (2010)
8. Yamashita, M., Fenn, J.B.: Electrospray ion source. another variation on the free-jet theme. J. Chem. Phys. **88**, 4451–4459 (1984)
9. Levin, D.S., Vouros, P., Miller, R.A., Nazarov, E.G.: Using a nanoelectrospray-differential mobility spectrometer-mass spectrometer system for the analysis of oligosaccharides with solvent selected control over ESI aggregate ion formation. J. Am. Soc. Mass Spectrom. **18**, 502–511 (2007)
10. Kang, Y., Terrier, P., Ding, C., Douglas, D.: Solution and gas-phase H/D exchange of protein–small-molecule complexes: cex and its inhibitors. J. Am. Soc. Mass Spectrom. **23**, 57–67 (2012)
11. Loo, J.A.: Studying noncovalent protein complexes by electrospray ionization mass spectrometry. Mass Spectrom. Rev. **16**, 1–23 (1997)
12. Guevremont, R., Purves, R.W.: High field asymmetric waveform ion mobility spectrometry-mass spectrometry: an investigation of leucine enkephalin ions produced by electrospray ionization. J. Am. Soc. Mass Spectrom. **10**, 492–501 (1999)
13. Bruins, A.P., Covey, T.R., Henion, J.D.: Ion spray interface for combined liquid chromatography/atmospheric pressure ionization mass spectrometry. Anal. Chem. **59**, 2642–2646 (1987)
14. Manisali, I., Chen, D.D., Schneider, B.B.: Electrospray ionization source geometry for mass spectrometry: past, present, and future. Trends Anal. Chem. **25**, 243–256 (2006)
15. Chowdhury, S.K., Katta, V., Chait, B.T.: An electrospray-ionization mass spectrometer with new features. Rapid Commun. Mass Spectrom. **4**, 81–87 (1990)
16. Mylchreest, I.C., Hail, M.E.: Electrospray ion source with reduced neutral noise and method. United States Patent RE35413 (1996)
17. Schneider, B.B., Baranov, V.I., Javaheri, H., Covey, T.R.: Particle discriminator interface for nanoflow ESI-MS. J. Am. Soc. Mass Spectrom. **14**, 1236–1246 (2003)
18. Schneider, B.B., Javaheri, H., Covey, T.R.: Ion sampling effects under conditions of total solvent consumption. Rapid Commun. Mass Spectrom. **20**, 1538–1544 (2006)
19. Mordehai, A., Buttrill, S.E.J.: Mass spectrometer system and method for transporting and analyzing ions. United States Patent 5672868 (1996)
20. Takada, Y., Sakairi, M., Hirabayashi, A., Ose, Y.: Mass spectrometer. United States Patent 5481107 (1996)
21. Dunyach, J.J., Specht, A.A., Atherton, R.P. Ion guide with improved gas dynamics and combined noise reduction device. United States Patent 8461524 (2013)
22. Michalski, A., Damoc, E., Lange, O., Denisov, E., Nolting, D., Mueller, M., Viner, R., Schwartz, J., Remes, P., Belford, M., Dunyach, J.J., Cox, J., Horning, S., Mann, M., Makarov, A.: Ultra high resolution linear ion trap Orbitrap mass spectrometer (Orbitrap Elite) facilitates top down LC MS/MS and Versatile peptide fragmentation modes. Mol. Cell. Proteom. **11**, O111.013698 (2012)
23. Mimura, T., Kato, Y., Matsumura, K.: Mass spectrometer. United States Patent 5298744 (1994)
24. Isenberg, S.L., Armistead, P.M., Glish, G.L.: Optimization of peptide separations by differential ion mobility spectrometry. J. Am. Soc. Mass Spectrom. **25**, 1592–1599 (2014)
25. Kanu, A.B., Dwivedi, P., Tam, M., Matz, L., Hill Jr., H.H.: Ion mobility-mass spectrometry. J. Mass Spectrom. **43**, 1–22 (2008)
26. Schneider, B.B., Covey, T.R., Coy, S.L., Krylov, E.V., Nazarov, E.G.: Planar differential mobility spectrometer as a prefilter for atmospheric pressure ionization mass spectrometry. Int. J. Mass Spectrom. **298**, 45–54 (2010)
27. Porta, T., Varesio, E., Hopfgartner, G.: Gas-phase separation of drugs and metabolites using modifier-assisted differential ion mobility spectrometry hyphenated to liquid extraction surface analysis and mass spectrometry. Anal. Chem. **85**, 11771–11779 (2013)
28. Jin, W., Jarvis, M., Star-Weinstock, M., Altemus, M.: A sensitive and selective LC-differential mobility-mass spectrometric analysis of allopregnanolone and pregnanolone in human plasma. Anal. Bioanal. Chem. **405**, 9497–9508 (2013)
29. Ray, J.A., Kushnir, M.M., Yost, R.A., Rockwood, A.L., Meikle, A.W.: Performance enhancement in the measurement of five endogenous steroids by LC-MS/MS combined with differential ion mobility spectrometry. Clin. Chim. Acta **438**, 330–336 (2015)
30. Krylov, E.V., Nazarov, E.G., Miller, R.A.: Differential mobility spectrometer: model of operation. Int. J. Mass Spectrom. **266**, 76–85 (2007)
31. Schneider, B.B., Nazarov, E.G., Londry, F., Vouros, P., Covey, T.R.: Differential mobility spectrometry/mass spectrometry history, theory, design optimization, simulations, and applications. Mass Spectrom. Rev. **35**, 687–737 (2015)
32. Schneider, B.B., Guo, X., Fell, L.M., Covey, T.R.: Stable gradient nanoflow LC-MS. J. Am. Soc. Mass Spectrom. **16**, 154–1551 (2005)
33. Canterbury, J.D., Yi, X., Hoopmann, M.R., MacCoss, M.J.: Assessing the dynamic range and peak capacity of nanoflow LC- FAIMS-MS on an ion trap mass spectrometer for proteomics. Anal. Chem. **80**, 6888–6897 (2008)